

Separating Electrons and Pions in MIPP using the Global Particle ID algorithm

Rajendran Raja¹

¹ *Fermi National Accelerator Laboratory*

Batavia, IL 60510

(Dated: July 3, 2010)

Abstract

MIPP uses dE/dx in its TPC, the Time of Flight system (TOF), the multi-cell Cerenkov (Ckov) and the Ring Imaging Cerenkov system (RICH) to identify final state charged particles in interactions. The TPC dE/dx is used for identification of e^\pm, π^\pm, K^\pm and p^\pm below 1 GeV/c momentum, the ToF below 2 GeV/c, the Ckov threshold is ≈ 2.5 GeV/c for pions and the RICH is capable of identifying particles that enter it up to 120 GeV/c. All particle id schemes depend on the value of β , the particle's velocity. Electrons are close to $\beta = 1$ for very low momenta and pions also reach near- $\beta=1$ status early on. This results in overlapping likelihoods for electrons and pions in all our detectors in significant regions of phase space. This note describes the importance of transverse momentum of the particle as an additional piece of information to be used in the likelihood scheme that results in a clean separation between electrons and pions in all of phase space.

I. GLOBAL PARTICLE IDENTIFICATION ALGORITHM

Let H denote the particle hypothesis. In our analysis we try and distinguish between e^\pm, π^\pm, K^\pm and p^\pm . Deuterons and higher mass nuclear fragments are not considered in this analysis but may be added on later. Let x denote the observed quantity from which particle identification is obtained. The symbol x can denote dE/dx in the TPC, time of flight in the TOF system, ADC values in the CKOV mirrors or the ring radii in the RICH. In addition, x can denote the p_t of the particle, since as we will show this contains information as to whether the particle is an electron or a hadron. We consider a track of momentum p . Then the joint probability that the track fits the hypothesis H and produces the observables x can be written as

$$P(H, x) = P(x|H)P(H) \quad (1)$$

where $P(H)$ is the probability that the particle is H and $P(x|H)$ is the probability that given H , the observables with values x is produced. Then by Bayes' theorem [1], this is also equal to

$$P(H|x)P(x) = P(H, x) = P(x|H)P(H) \quad (2)$$

summing over hypotheses H , one gets

$$\sum_H P(H|x)P(x) = \sum_H P(x|H)P(H) \quad (3)$$

since $\sum_H P(H) = 1$ and $\sum_H P(H|x) = 1$ by unitarity, this leads to

$$P(H|x) = \frac{P(x|H)P(H)}{\sum_H P(x|H)P(H)} \quad (4)$$

The denominator $\sum_H P(x|H)P(H)$ of above equation is the total likelihood that of observing the quantity x given a prior possibility $P(H)$ of hypothesis H and a conditional likelihood $P(x|H)$ of observing H . This may be written as a weight $wt(H)$ for a given event H

$$P(H|x) = \frac{wt(H)}{\sum_H wt(H)} \quad (5)$$

where

$$wt(H) = P(x|H)P(H) \quad (6)$$

The posterior probability $P(H|x)$ is the probability that the track with observables fits the hypothesis H. The prior probability $P(H)$ is initially unknown and represents the fraction of the sample that belong to each hypothesis. See ref [2] for a determination of priors in ionization data.

A. Iterative determination of the prior probabilities

At the first iteration $P(H)$ is set to $1/n_H$ where n_H is the number of hypotheses (in our case 4). i.e. initially all hypotheses are set to have equal probabilities. We then loop over all detectors and tracks calculating the likelihood $P(x|H)$ for each detector. The overall likelihood for a track that goes through multiple detectors is given by the product of the individual likelihoods.

$$P(\vec{x}|H) = \prod_{i=1}^{i=ndet} P(x_i|H) \quad (7)$$

The quantity \vec{x} denotes the set of observables from multiple detectors. At the end of the first iteration each track is weighted by $P(H|x)$ for the hypothesis H. If $P(H|x)$ is unity, then the track is uniquely identified as that hypothesis and will be considered only for that hypothesis. In practice events often have $P(H|x)$ that are close to unity. They will then enter multiple histograms with appropriate weights. The new values of $P(H)$ are used to iterate over the events again and the process is repeated until we have convergence for $P(H)$. We find that ≈ 15 iterations are needed for convergence. After convergence, $P(H)$ will yield the momentum spectrum for each hypothesis since the above formalism applies for each track of momentum p .

II. GLOBAL PID ANALYSIS OF NUMI TARGET

Figure 1 shows the momentum spectrum of charged particles detected in MIPP on the full NuMI target. The incident beam is 120 GeV/c protons from the Main Injector. We recorded ≈ 1.8 Million events on NuMI target. We have analyzed a fraction of these for this note (in the interests of speed). The bump at 120 GeV/c is due to primary protons that punch through the NuMI target without interaction but are tracked by MIPP with a momentum resolution $\delta p/p = 5\%$.

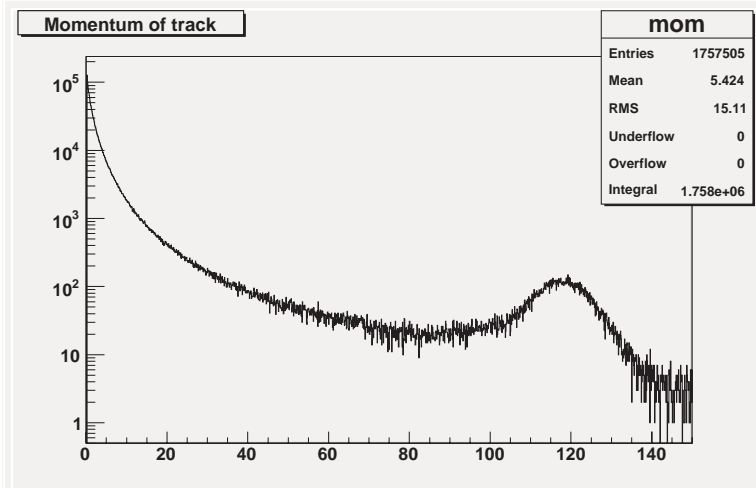


FIG. 1: The reconstructed momentum of all secondary tracks measured in MIPP with 120 GeV/c protons incident on the NuMI target. The bump at 120 GeV/c are the protons that punch through the NuMI thick target without interacting.

III. THE ROLE OF TRANSVERSE MOMENTUM IN ELECTRON PION SEPARATION

Electrons and pions are near $\beta = 1$ over a large fraction of phase space and are difficult to distinguish. However electrons arise from the conversion of photons which arise from the decay of π^0 particles. Charged pions and π^0 's are produced with the same p_t distribution. When a π^0 decays into two photons, each photon on average will have half the energy of the π^0 . The average direction of each photon will be roughly the same as the π^0 direction. The p_t of the photon will on average be \approx half that of the π^0 purely due to the division of the momentum. This process repeats itself when the photon converts to produce the electron-positron pair. The electrons (and positrons) will have half the p_t of the parent photon on average and thus will have 1/4 the p_t of the charged and neutral pions. We illustrate this using NuMI data. Figure 2 shows the radii of secondary charged particles from the NuMI target as a function on particle momentum in the MIPP RICH. The pions are above RICH threshold above ≈ 5 GeV/c. There is a strong electron band at $\beta=1$ radius of 30 cm right down to 2 GeV/c. If we choose RICH particles below 3 GeV/c as “golden electrons” (i.e. not contaminated by pions) and plot the p_t^2 spectrum and compare it against the pion spectrum, the two curves as shown in Figure 3 result. The electron p_t^2 spectrum falls steeply. There

are no electrons with $p_t^2 > 0.2$. The pion p_t^2 spectrum is much flatter and extends beyond 1.5 (GeV/c)². Both curves are normalized to unity and can be used as additional functions for calculating the likelihood $P(x|H)$. Figure 4 shows the electron spectrum in the RICH with

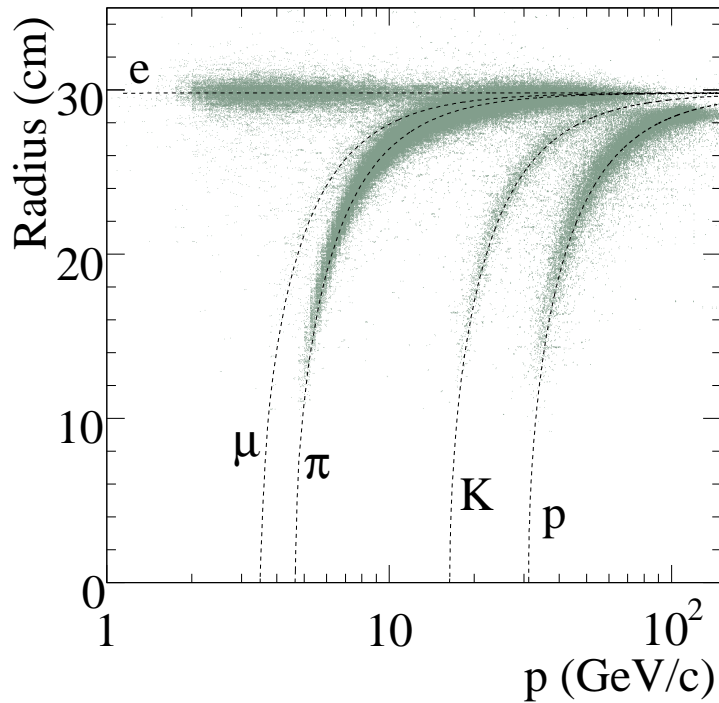


FIG. 2: Ring radii as a function of momentum for particle coming from the NuMI target in MIPP.

and without p_t^2 weighting. The blue curve is without p_t^2 weighting and shows a significant “leak” of pions into the electron channel due to statistical fluctuation above 20 GeV/c momentum. With p_t^2 weighting, the red curve results and the correct electron spectrum is obtained. This method can be extended to all the MIPP detectors and results in clean electron pion separation throughout phase space.

Figure 5 shows the transverse momentum spectrum of all the charged particles in MIPP from the NuMI target. A strong electron peak at low p_t is evident indicating conversion of photons in the target material. Figure 6 shows the likelihood for electrons and pions after the application of the p_t^2 likelihood in addition to the other detectors [3]. The left hand plot of Figure 6 shows the electron p_t and the right hand plot shows the pion p_t . A clean separation between the two particles is obtained. Figure 7 shows the NuMI target data in the TPC in the momentum range of interest. We analyze the TPC dEdx from 0.2-1.0 GeV/c. The vertical axis is $\log_e(dEdx)$. The dEdx units are normalized so that the

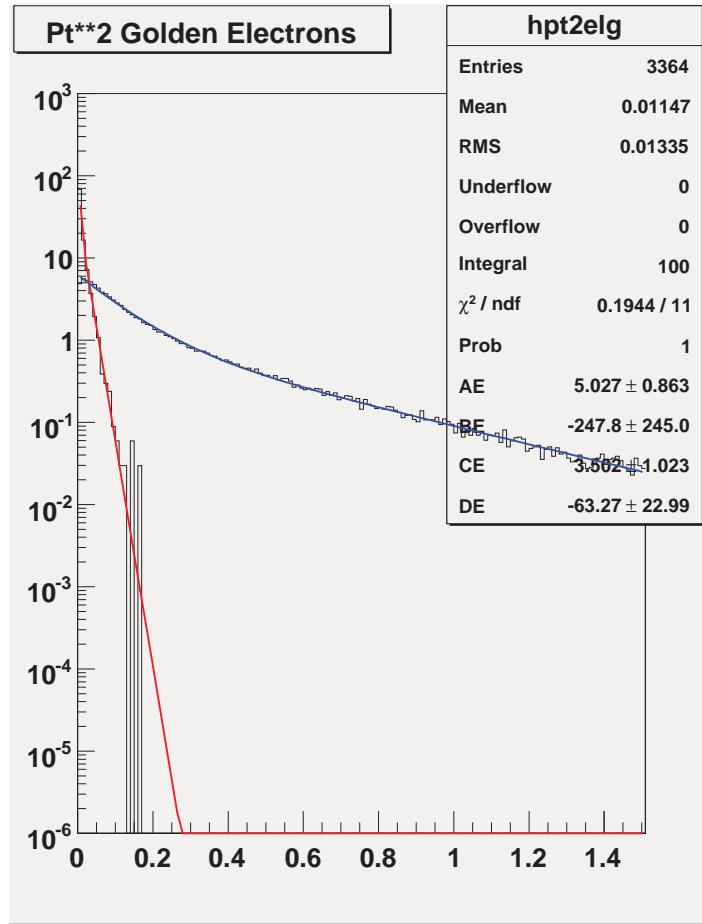


FIG. 3: Red curve shows p_t^2 distribution of “golden” electrons as identified by RICH (momentum $< 3 \text{ GeV}/c$) which are below pion threshold. The red curve shows the distribution of pions. Both curves are normalized to unity.

pion average dE/dx is unity in the momentum range of interest. A strong electron peak at $\log_e(dE/dx)=0.5$ is evident. The TPC does separate electrons and pions by dE/dx , since electrons have on average higher deposition of ionization energy although some confusion results due to statistical fluctuation. Application of the p_t^2 likelihood in addition to the dE/dx likelihood will cleanly separate the two particles types. The same conclusions apply for the ToF and the Ckov.

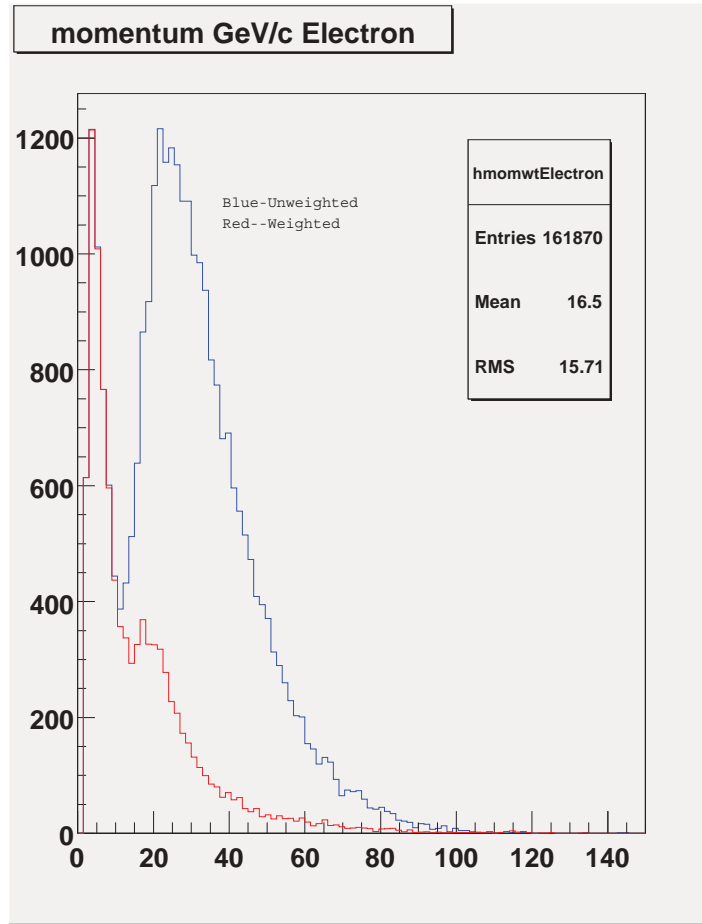


FIG. 4: Blue curve shows the momentum spectrum of tracks that solve as having best electron likelihood using RICH radii information only. One can see that there is a significant pion “leakage” into the electron channel (second bump at 25 GeV/c). Red curve shows the momentum spectrum of tracks that solve as electrons using RICH ring radii likelihood and p_t^2 likelihood.

IV. MONTE CARLO SIMULATION OF THE NUMI TARGET

The NuMI target was simulated using FLUKA by the NuMI group. The particle 4 vectors leaving the surface of the target volume were handed over to MIPP in format appropriate for Geant simulation. The Geant3 based MIPP simulation program E907MC was used to track the particles in the MIPP apparatus. The TPC was modeled in great detail including missing and dead channels. Figure 8 shows the p_t spectrum of charged particles resulting from such a Monte Carlo simulation. There is a significant deficit of conversion electrons

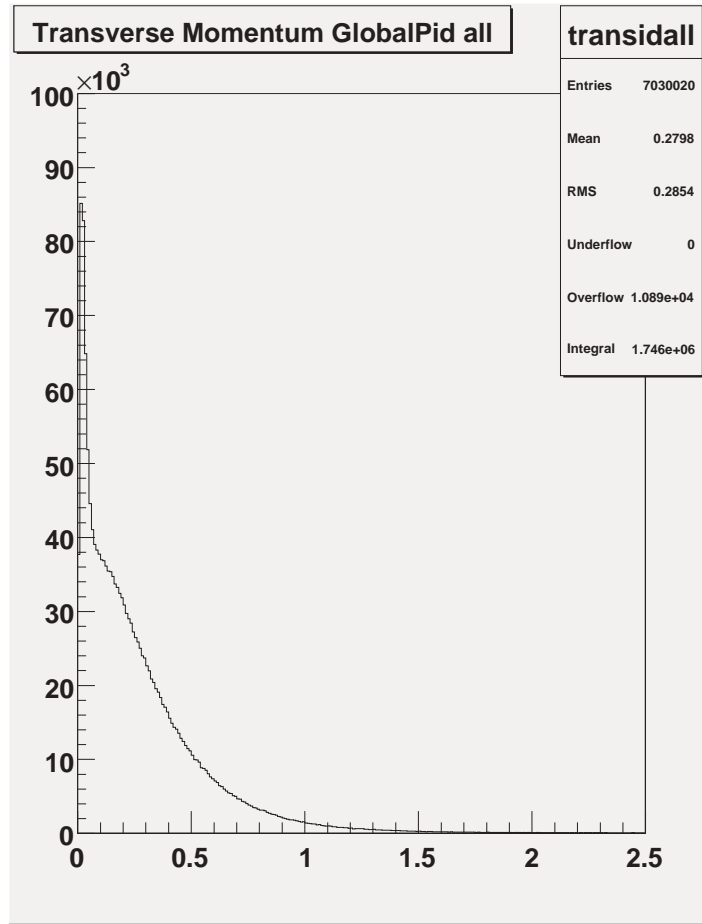


FIG. 5: The reconstructed transverse momentum of secondary tracks measured in MIPP with 120 GeV/c protons incident on the NuMI target. The bump at low p_t is due to large number of conversion electrons produced in the NuMI target.

in the Monte Carlo when compared to corresponding Figure 5 from NuMI data. Figure 9 shows the $\log(dE/dx)$ distributions as a function of momentum for the NuMI Monte Carlo events in the MIPP simulated TPC. There again is a clear deficit of conversion electrons in the simulated events when compared to the data as in Figure 7. Figure 10 shows the comparison of p_t^2 distribution of electrons and pions generated in the NuMI Monte Carlo simulation. This can be compared to Figure 4 which used identified electrons in the RICH to reach the same conclusion. We plan shortly to use the NuMI Monte Carlo to provide more detailed pt^2 likelihood curves.

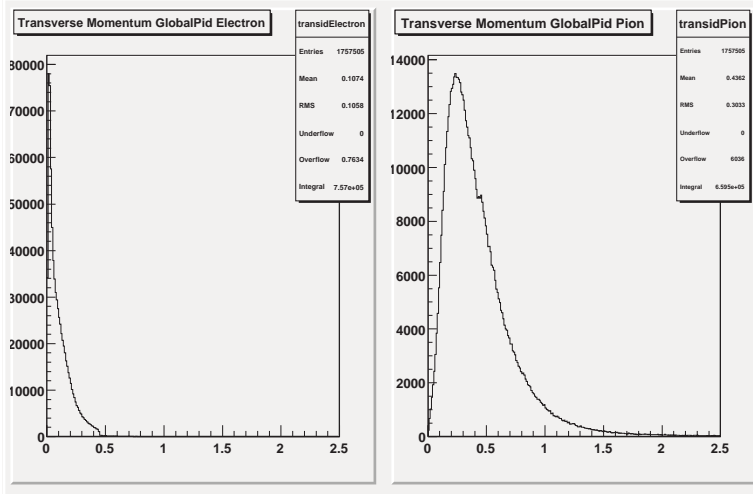


FIG. 6: The left hand plot shows the electron transverse momentum after p_t weighting. The right hand plot shows the pion transverse momentum after p_t weighting. Data is NuMI target. Horizontal axes are in GeV/c.

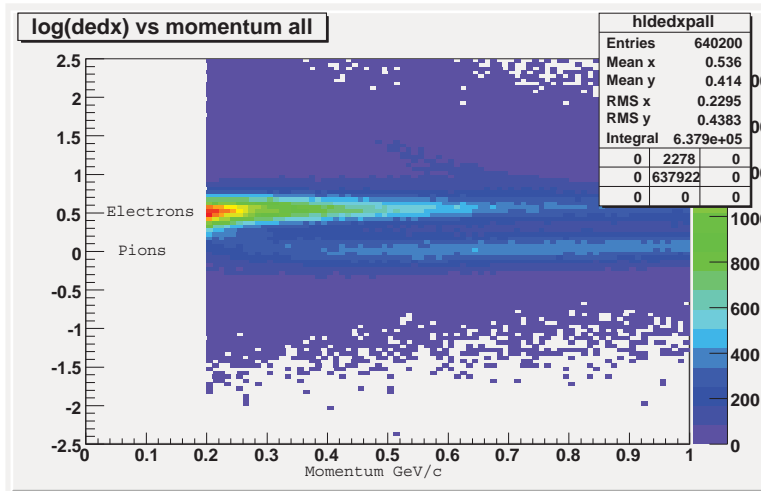


FIG. 7: NuMI data in the TPC. Vertical axis shows the $\log(\text{dedx})$, where the units are such that the pion dedx is normalized to unity. Horizontal axis is from 200 MeV/c to 1 GeV/c, our range of analysis for NuMI data in the TPC.

V. CONCLUSION

We have described a new likelihood method that adds p_t of the particle as an additional piece of information to separate electrons and pions. It provides a powerful new tool to be used in conjunction with the particle id apparatus of MIPP. There is a significant excess

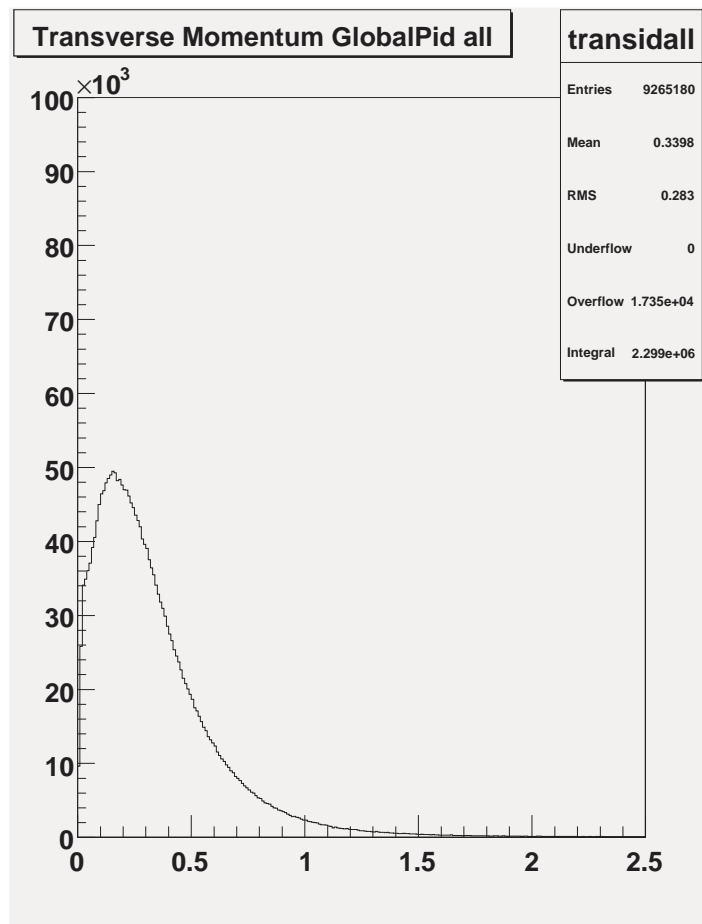


FIG. 8: The reconstructed transverse momentum of secondary tracks in NuMI Monte Carlo. The slight enhancement at low p_t is due to conversion electrons in the NuMI target in the Monte Carlo. This is much less pronounced than in data (see Figure 5)

in the number of conversion electrons produced in NuMI target data when compared to the NuMI FLUKA Monte Carlo (simulation performed by NuMI). This is very likely due to additional material in the NuMI target not present in the simulation. Whether this translates into differences in charged particles will be revealed by further analysis of MIPP data.

[1] “An essay towards solving a problem in the doctrine of chances”, Rev. Thomas Bayes, *Biometrika*, **45** 293-315 (Reprint of 1763) (1958).

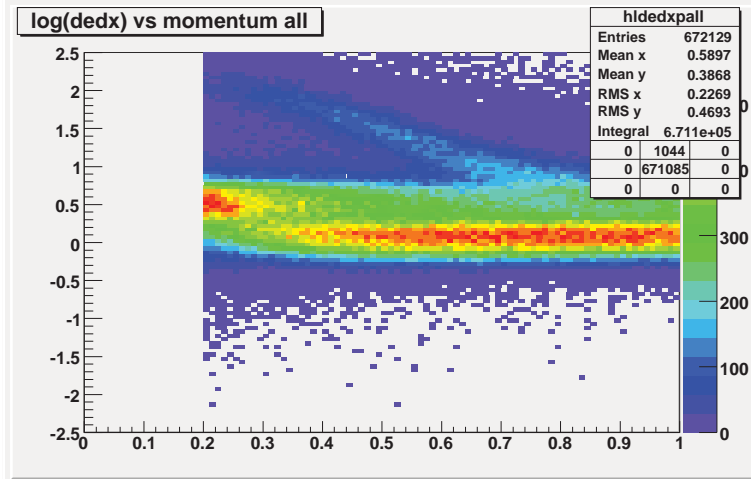


FIG. 9: NuMI Monte Carlo in the TPC. Vertical axis shows the $\log(\text{dedx})$, where the units are such that the pion dedx is normalized to unity. Horizontal axis is from 200 MeV/c to 1 GeV/c, our range of analysis for NuMI data. The NuMI Monte Carlo has far fewer electrons than the NuMI data. This implies that the NuMI target material is not well represented in the NuMI Monte Carlo.

[2] “Maximum Likelihood Analysis of Ionization Data from SAMM”, R. Raja, D. Bogert NIM 143:543, 1977.

[3] We are in the process of adding the Ckov to the detector mix.

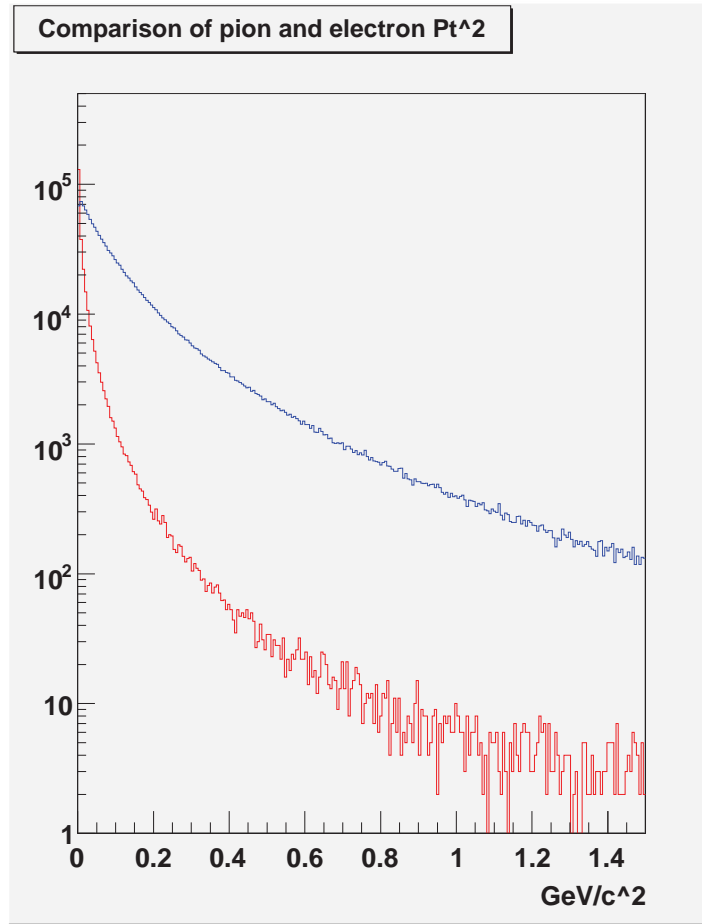


FIG. 10: Comparison of p_t^2 distribution of electrons (red) and (pions) from the Monte Carlo simulation of the NuMI target. This shows the same pt^2 effect as was evident from the particles from NuMI data as shown in Figure 4. Electrons have significantly narrower pt^2 distribution than pions.